Preparation and characterization of gold nanoparticles with a ruthenium-terpyridyl complex, and electropolymerization of their pyrrole-modified metal nanocomposites

Masayuki Ito, Takashi Tsukatani and Hisashi Fujihara*

Received 11th August 2004, Accepted 25th November 2004
First published as an Advance Article on the web 5th January 2005
DOI: 10.1039/b412406e

The reduction of tetrachloroaurate with sodium borohydride in the presence of 2,2′:6′,2″-terpyridyloctanethiol gave terpyridine-functionalized gold nanoparticles (Tpy–Au, core size 2.0 nm). Metal complexation of Tpy–Au with ruthenium-terpyridyl trichloride, Ru(tpy)Cl_3, led to new gold nanoparticles bearing the ruthenium-terpyridine complex (Ru–Tpy–Au, core size 5.5 nm) which showed a characteristic MLCT (metal-to-ligand charge transfer) band in the visible region at 483 nm due to the terpyridine-ruthenium complex and a plasmon resonance at ~510 nm in the UV-vis spectrum. The redox behavior of Ru–Tpy–Au was studied by cyclic voltammetry. Surface modification of metal electrodes was performed by the electropolymerization of pyrrole-functionalized Ru–Tpy–Au nanoparticles (Pyr–Ru–Tpy–Au) which were obtained from the ligand-exchange reaction of Ru–Tpy–Au with ω-(*N*-pyrrolyl)decanethiol.

Introduction

Currently, noble metal particles on the nanometer scale represent a rapidly emerging field of great fundamental and practical interest and are receiving worldwide attention.[1–3] A number of gold nanoparticles containing functional units have been synthesized.[4,5] Functionalization of the gold nanoparticles with self-assembled monolayers provides a method for introducing diverse functionality to the nanoparticle surface. We recently reported the first preparation of fullerenethiolate-functionalized gold nanoparticles as new metal–C_{60} nanocomposites which are adsorbed onto the surface of gold electrodes to form nanoparticle films.[6] In contrast, much less attention has been paid to the preparation of functionalized gold nanoparticles with metal complexes. An intriguing further development in this area involves the attachment of electropolymerizable groups at the periphery of metal nanoparticles taking advantage of the electropolymerization process to prepare electrodes modified by electroactive poly(metal nanoparticles). Electrochemical polymerization is an elegant strategy for the immobilization of redox-active groups on the surface of electrodes and the preparation of conductive polymer thin films. The surface modification of electrodes with electroactive polymer thin films has been performed from the electrochemical polymerization of pyrrole-based monomers which are the most commonly used materials.[7] Recently, increasing attention is being given to the fabrication of thin films of metal nanoparticles from both a fundamental and a practical application point of view.[8] Such thin films of metal nanoparticles on solid surfaces have been prepared using a number of strategies including assembly techniques with crosslinkers for metal nanoparticles;[8] however, the literature on polymer thin films of metal nanoparticles by the electropolymerization method is quite limited.[9,10] This paper presents the preparation and characterization of gold nanoparticles (Tpy–Au) stabilized directly by 2,2′:6′,2″-terpyridinyloctanethiol (Tpy–SH: **1**) and their gold nanoparticles containing ruthenium-terpyridyl complexes (Ru–Tpy–Au) as a new class of metal nanocomposites. We also describe the surface modification of metal electrodes with pyrrole-functionalized Ru–Tpy–Au nanoparticles (Pyr–Ru–Tpy–Au) by electropolymerization. Terpyridines (Tpy) as chelating binding units and their ruthenium complexes are widely used for the construction of dendrimers as nanoscale-molecules and supramolecules because of their unique electrochemical and photochemical properties.[11]

Experimental

1. Chemicals

All reagents were purchased from Wako Pure Chemical Industries Ltd., Tokyo Kasei Co. Ltd., Fluka Chemical Co., or Aldrich Chemical Co. The reagents used as reaction solvents were further purified by general methods.

2. Instruments

NMR spectra were recorded on JEOL GSX270 and JEOL GSX500 (270 MHz and 500 MHz) spectrometers. UV-vis spectra were measured with a Hitachi U-4000. Mass spectra were recorded on a JEOL JMS-700. Fourier Transform Infrared (FT-IR) spectra were collected with a JASCO FT-IR-470. Transmission electron microscopy (TEM) measurements were performed on a JEOL JEM-3010. Samples for TEM studies were prepared by placing drops of the gold nanoparticles (Tpy–Au, Ru–Tpy–Au and Pyr–Ru–Tpy–Au) on carbon-coated TEM grids.

Cyclic voltammetry was performed at room temperature using a BAS Instrument model 100B/W electrochemical workstation. Platinum wire was used as the counter electrode

---

*h-fuji@apch.kindai.ac.jp

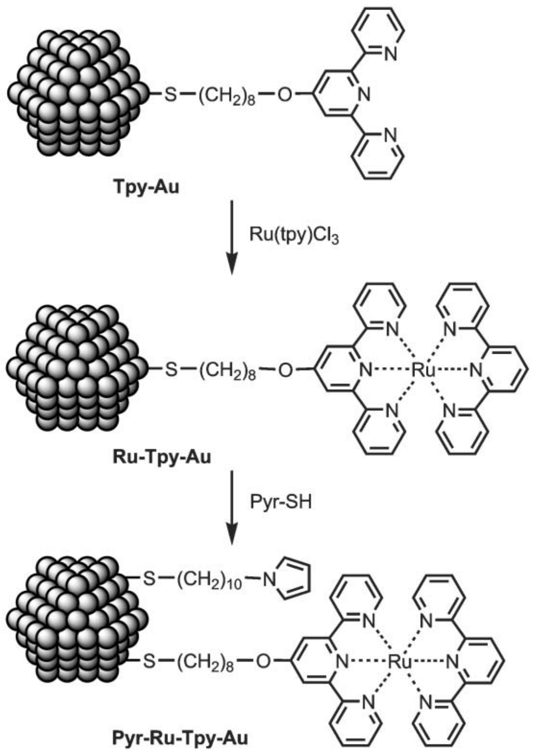

Scheme 1 Preparation of Ru–Tpy–Au and Pyr–Ru–Tpy–Au.

and glassy carbon (3.0 mm diameter) or gold (1.6 mm diameter) was used as the working electrode in a one-compartment cell. Potentials were relative to the system Ag/0.1 M $AgNO_3$ in acetonitrile. Bu_4NPF_6 (Fluka, electrochemical grade) and MeCN (Wako, anhydrous) were used for the preparation of electrolyte solutions.

3. Synthesis of terpyridine-thiol (1) and pyrrole-thiol (2)

The synthetic sequence is described in Schemes 2 and 3. 2,6-Bis(2′-pyridyl)-4-pyridone (**3**) was synthesized according to the procedure of Constable and Ward.[12]

4′-(8-Bromooctyloxy)-2,2′:6′,2″-terpyridine (**4**). A mixture of 2,6-bis(2′-pyridyl)-4-pyridone (**3**) (5.00 g, 20 mmol) and 1,8-dibromooctane (7.40 mL, 40 mmol) in the presence of K_2CO_3 (2.76 g, 20 mmol) in MeCN was stirred at reflux under argon for 16 h. After work-up, the crude products were purified by silica-gel column chromatography (benzene) to give **4**. **4**: mp 92–93 °C, ^1H NMR ($CDCl_3$) δ 8.72–8.67 (m, 2H, ArH), 8.65–8.58 (m, 2H, ArH), 8.00 (s, 2H, ArH), 7.88–7.80 (m, 2H, ArH), 7.36–7.29 (m, 2H, ArH), 4.22 (t, 2H, J = 7 Hz, OCH_2), 3.42 (t, 2H, J = 7 Hz, CH_2Br) and 1.88–1.30 (m, 12H, CH_2); ^{13}C NMR ($CDCl_3$) δ 167.3, 157.0, 156.2, 149.0, 136.7, 123.7, 121.3, 107.4, 68.1, 33.9, 32.8, 29.1, 28.9, 28.6, 28.1, 25.8. MS, m/z 440 (M^+).

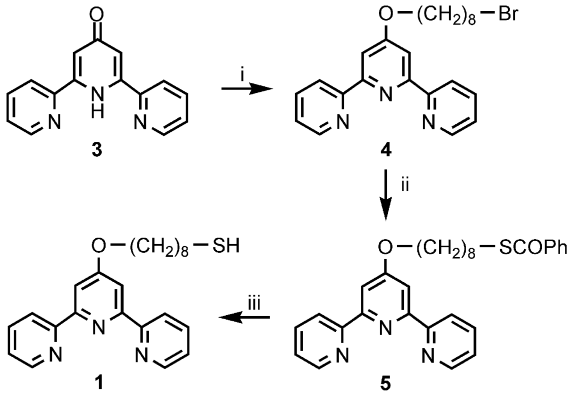

Scheme 2 *Reagents and conditions*: i, $Br(CH_2)_8Br$, K_2CO_3, MeCN, reflux; ii, PhCOSNa, MeCN, reflux; iii, $LiAlH_4$, THF, room temp.

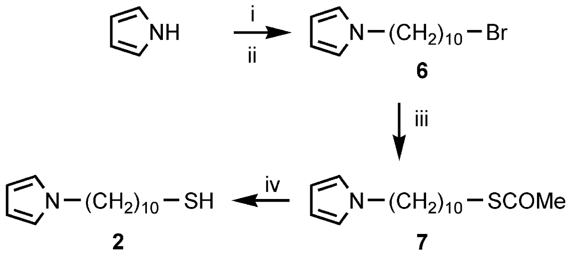

Scheme 3 *Reagents and conditions*: i, *n*-BuLi, THF, 0 °C; ii, $Br(CH_2)_{10}Br$, reflux; iii, MeCOSK, MeCN, room temp.; iv, HCl, MeOH, reflux.

4′-(8-Thiobenzoateoctyloxy)-2,2′:6′,2″-terpyridine (**5**). A mixture of **4** (2.20 g, 5 mmol) and sodium thiobenzoate (1.12 g, 7 mmol) in anhydrous MeCN (80 mL) was refluxed for 13 h. After work-up, the crude products were recrystallized from MeCN to give **5**. **5**: mp 98 °C; FT-IR 1661 cm^{-1} (C=O); ^1H NMR ($CDCl_3$) δ 8.70–8.67 (m, 2H, ArH), 8.64–8.59 (m, 2H, ArH), 8.01 (s, 2H, ArH), 7.98–7.95 (m, 1H, ArH), 7.87–7.80 (m, 2H, ArH), 7.56–7.53 (m, 1H, ArH), 7.46–7.43 (m, 1H, ArH), 7.35–7.32 (m, 1H, ArH), 4.24 (t, 2H, J = 7 Hz, OCH_2), 3.08 (t, 2H, J = 7 Hz, SCH_2), 1.90–1.38 (m, 12H, CH_2); ^{13}C NMR ($CDCl_3$) δ 192.1, 167.3, 157.0, 156.2, 149.0, 137.2, 136.7, 133.1, 128.5, 127.1, 123.7, 121.3, 107.4, 68.1, 29.5, 29.1, 29.0, 28.95, 28.9, 28.8, 25.8. MS, m/z 498 (M^+).

4′-(8-Mercaptooctyloxy)-2,2′:6′,2″-terpyridine (Tpy–SH: **1**). A mixture of **5** (996 mg, 2 mmol) and $LiAlH_4$ (152 mg, 4 mmol) in anhydrous THF (30 mL) was stirred under argon at room temperature for 5 h. After work-up, the crude products were purified by alumina column chromatography (hexane–$MeCO_2Et$ = 10 : 1) to give **1**. **1**: mp 73–74 °C; FT-IR 2510 cm^{-1} (SH); ^1H NMR ($CDCl_3$) δ 8.71–8.67 (m, 2H, ArH), 8.64–8.59 (m, 2H, ArH), 8.01 (s, 2H, ArH), 7.88–7.81 (m, 2H, ArH), 7.36–7.30 (m, 2H, ArH), 4.22 (t, 2H, J = 7 Hz, OCH_2), 2.53 (dt, 2H, J = 8, 7 Hz , CH_2S), 1.86 (q, 2H, J = 7 Hz, CH_2), 1.68–1.40 (m, 10H, CH_2), 1.35 (t, 1H, J = 8 Hz, SH); ^{13}C NMR ($CDCl_3$) δ 167.3, 157.0, 156.1, 149.0, 136.7, 123.7, 121.3, 107.3, 68.1, 34.0, 29.1, 28.9, 28.2, 25.8, 24.6. MS, m/z 393 (M^+).

1-(10-Bromodecyl)pyrrole (**6**). A mixture of pyrrole (5 mL, 72 mmol) and *n*-BuLi (1.6 M/hexane, 56 mL, 90 mmol) in anhydrous THF was stirred at 0 °C under argon for 1 h. Then, 1,10-dibromodecane (16 mL, 72 mmol) in anhydrous was added dropwise. This mixture was refluxed for 2 h. After work-up, the crude products were purified by silica-gel column chromatography (hexane–benzene = 1 : 1) to give **6**. **6**: ^1H

NMR ($CDCl_3$) δ 6.64 (t, 2H, J = 2 Hz, 2,5-pyrrole), 6.13 (t, 2H, J = 2 Hz, 3,4-pyrrole), 3.86 (t, 2H, J = 7 Hz, NCH_2), 3.40 (t, 2H, J = 7 Hz, CH_2Br), 1.85 (q, 2H, J = 7 Hz, $BrCH_2CH_2$), 1.75 (q, 2H, J = 7 Hz, NCH_2CH_2) and 1.41–1.22 (m, 12H, CH_2); ^{13}C NMR ($CDCl_3$) δ 120.4, 107.7, 49.6, 34.0, 32.8, 31.5, 29.3, 29.2, 29.1, 28.7, 28.1 and 26.7. MS, *m*/*z* 286 (M^+).

1-(10-Thioacetyldecyl)pyrrole (**7**). A mixture of **6** (552 mg, 1.93 mmol) and potassium thioacetate (440 mg, 3.85 mmol) in anhydrous MeCN (12 mL) was stirred at room temperature under argon for 2 h. After work-up, the crude products were purified by silica-gel column chromatography (hexane–benzene = 1 : 3) to give **7**. **7**: FT-IR 1692 cm^{-1} (C=O); ^{1}H NMR ($CDCl_3$) δ 6.64 (t, 2H, J = 2 Hz, 2,5-pyrrole), 6.13 (t, 2H, J = 2 Hz, 3,4-pyrrole), 3.85 (t, 2H, J = 7 Hz, NCH_2), 2.85 (t, 2H, J = 7 Hz, CH_2S), 2.31 (s, 3H, CH_3), 1.75 (q, 2H, J = 7 Hz, NCH_2CH_2), 1.55 (q, 2H, J = 7 Hz, SCH_2CH_2) and 1.40–1.20 (m, 12H, CH_2); ^{13}C NMR ($CDCl_3$) δ 196.0, 120.4, 107.7, 49.5, 31.5, 29.4, 29.3, 29.2, 29.1, 29.0, 28.7 and 26.7. MS, *m*/*z* 281 (M^+).

1-(10-Mercaptodecyl)pyrrole (Pyr–SH: **2**). A mixture of **7** (223 mg, 0.793 mmol) and 3 N HCl (0.4 mL) in MeOH (9 mL) was refluxed for 2 h. After work-up, the crude products were purified by silica-gel column chromatography (benzene) to give **2**. **2**: FT-IR 2554 cm^{-1} (SH); ^{1}H NMR ($CDCl_3$) δ 6.64 (t, 2H, J = 2 Hz, 2,5-pyrrole), 6.13 (t, 2H, J = 2 Hz, 3,4-pyrrole), 3.85 (t, 2H, J = 7 Hz, NCH_2), 2.51 (dt, 2H, J = 8, 7 Hz, CH_2SH), 1.75 (q, 2H, J = 7 Hz, NCH_2CH_2), 1.59 (q, 2H, J = 7 Hz, SCH_2CH_2), 1.42–1.23 (m, 12H, CH_2) and 1.32 (t, 1H, J = 8 Hz, SH); ^{13}C NMR ($CDCl_3$) δ 120.4, 107.7, 49.7, 49.6, 33.9, 31.5, 29.3, 29.1, 28.9, 28.3, 26.7 and 24.5. MS, *m*/*z* 239 (M^+).

4. Preparation of Tpy–Au, Ru–Tpy–Au and Pyr–Ru–Tpy–Au nanoparticles

Preparation of Tpy–Au. To a vigorously stirred solution of tetraoctylammonium bromide (3.84 g, 7.02 mmol) in 90 mL of toluene was added $HAuCl_4\cdot 4H_2O$ (650 mg, 1.58 mmol) in 60 mL of deionized water. A solution of a thiol **1** (581 mg, 1.48 mmol) in 50 mL of toluene was added, and the resulting solution was stirred for 20 min at room temperature. $NaBH_4$ (662 mg, 17.5 mmol) in 40 mL of deionized water was then added. The mixture was stirred for 3 h at room temperature. After stirring the organic phase was evaporated to 20 mL in *vacuo* and mixed with EtOH (800 mL). The resulting precipitate was collected by filtration and washed several times with EtOH. The nanoparticles were redissolved in $CHCl_3$ to purify and precipitated with EtOH, and then the particles were isolated by filtration. These processes were repeated until no free thiol or phase transfer catalyst remained, as detected by TLC and ^{1}H and ^{13}C NMR spectroscopy.

Preparation of Ru–Tpy–Au. Metal complexation of the Tpy–Au nanoparticle ligands was achieved by the following procedure. Ru(tpy)Cl_3 was obtained according to the literature.[13] A mixture of Tpy–Au nanoparticles (50 mg) in $CHCl_3$ (5 mL) and Ru(tpy)Cl_3 (23 mg) in EtOH–H_2O (1 : 1, 200 mL) was refluxed for 24 h. After stirring, the solution was condensed in *vacuo* and mixed with diethyl ether. An aqueous solution of NH_4PF_6 was then added to precipitate the terpyridine-ruthenium complexes, Ru–Tpy–Au nanoparticles.

Preparation of Pyr–Ru–Tpy–Au. The ligand-exchange reaction of Ru–Tpy–Au with a pyrrolethiol **2** was carried out as follows. A mixture of Ru–Tpy–Au nanoparticles (50 mg) and thiol **2** (15 mg) in MeCN (2 mL) was stirred at room temperature for 48 h. To the mixture was added EtOH (200 mL) and then the resulting precipitate was collected by filtration and washed several times with EtOH. The nanoparticles were redissolved in MeCN to purify and precipitated with EtOH, and then the particles were isolated by filtration.

Results and discussion

Terpyridine-functionalized gold nanoparticles (Tpy–Au) were prepared by the two-phase reaction[4] and repeatedly isolated from and redissolved in organic solvents and extremely stable. Metal complexation on the nanointerface of Tpy–Au with Ru(tpy)Cl_3 led to the formation of Ru–Tpy–Au nanoparticles. New redox-active multifunctional gold nanoparticles (Pyr–Ru–Tpy–Au) containing Ru-terpyridine complexes and pyrrole groups as electropolymerization sites were obtained from the ligand-exchange reaction[5] of Ru–Tpy–Au with a pyrrole-substituted decanethiol (**2**) (Scheme 1).

The UV-vis spectrum of the Tpy–Au nanoparticle solution in $CHCl_3$ exhibited a small plasmon resonance at ~505 nm, which means the formation of small gold nanoparticles [Fig. 1(inset)]. Further characterization of the material was performed with use of NMR spectroscopy and transmission electron microscopy (TEM). The proton signals in the ^{1}H NMR spectrum of Tpy–Au, though significantly broadened, appeared at positions that are almost identical to those of free thiol **1**.[14] The ^{13}C NMR spectrum of Tpy–Au in $CDCl_3$ showed the peaks of non-coordinate terpyridine ligands at

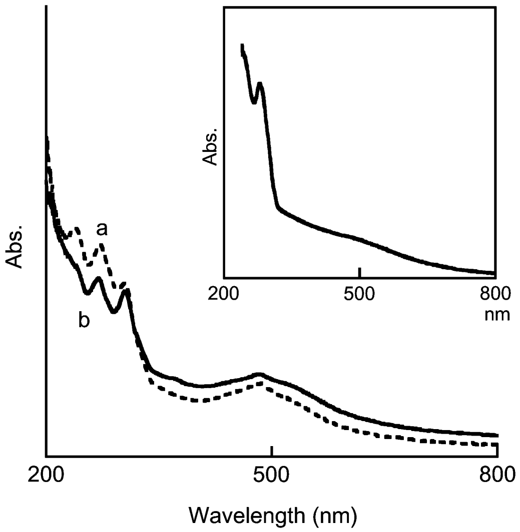

Fig. 1 UV-vis spectra of (a) Ru–Tpy–Au in MeCN and (b) Pyr–Ru–Tpy–Au in MeCN. Inset: Tpy–Au in $CHCl_3$.

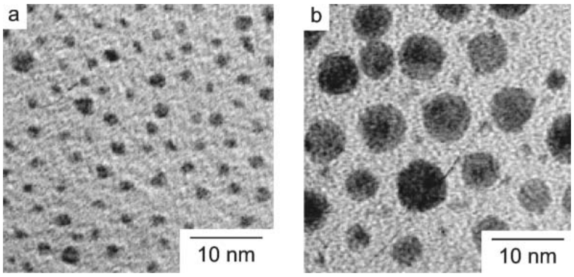

Fig. 2 TEM micrographs of (a) Tpy–Au and (b) Ru–Tpy–Au.

δ 167.0, 156.6, 155.7, 148.8, 136.4, 123.5, 121.0 and 107.2 which are consistent with those of **1**. The core size obtained from TEM images of Tpy–Au is found to be 2.0 ± 0.4 nm [Fig. 2(a)].

Evidence for complexation of Tpy–Au with Ru(tpy)Cl_3 was provided by NMR and UV-vis spectroscopy, and electrochemical data. The ^{13}C NMR spectrum of Ru–Tpy–Au in CD_3CN showed significant doubling of the terpyridine peaks at δ 167.5, 159.3, 159.1, 156.95, 156.92, 153.7, 153.3, 138.93, 138.87, 136.2, 128.45, 128.41, 125.4, 125.3, 124.6 and 112.0. The UV-vis spectrum of Ru–Tpy–Au in MeCN showed a characteristic MLCT (metal-to-ligand charge transfer) transition in the visible region at 483 nm [Fig. 1(a)], indicating the formation of a terpyridine-ruthenium complex.[11] The absorption maximum at 306, 273 and 242 nm is also distinctive. Furthermore, Fig. 1(a) shows that the plasmon resonance at ~510 nm is bigger than that of Tpy–Au shown in Fig. 1(inset), which means the formation of large particles in comparison with Tpy–Au. The result of the UV-vis spectrum is in good agreement with that obtained from the TEM micrograph of Ru–Tpy–Au, *i.e.*, Fig. 2(b) shows an increase in the particle size by addition of Ru(tpy)Cl_3 with heating. The particle size of Ru–Tpy–Au is 5.5 ± 1.0 nm as measured by TEM [Fig. 2(b)]. This finding indicates that Tpy–Au undergoes aggregation into somewhat large particles upon addition of Ru(tpy)Cl_3. This aggregation seems to be due to heating of the gold nanoparticles.[15]

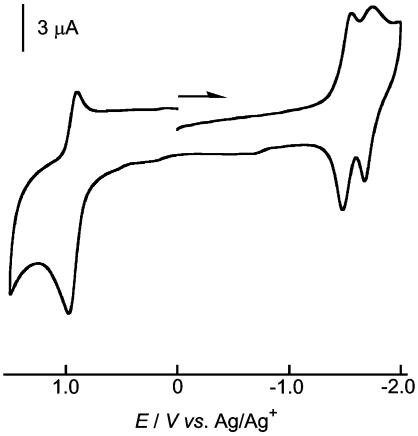

Fig. 3 Cyclic voltammogram of Ru–Tpy–Au on a GC electrode in 0.1 M Bu_4NPF_6–MeCN; scan rate 100 mV s^{-1}.

The electrochemical properties of Ru–Tpy–Au were studied by cyclic voltammetry. The cyclic voltammogram of Ru–Tpy–Au was measured in 0.1 M Bu_4NPF_6–MeCN at a glassy carbon electrode and Ag/0.1 M $AgNO_3$ reference electrode (scan rate: 100 mV s^{-1}). The half-wave potentials ($E_{1/2}$) and the cathodic–anodic peak separation (ΔEp) values for two terpyridine redox processes and the ruthenium(II)/(III) process showed the following values: $E_{1/2} = -1.52$ (ΔEp = 74) and −1.71 V (ΔEp = 52 mV) for tpy ligands, and +0.93 V (ΔEp = 62 mV) for the Ru(II)/(III) couple (Fig. 3). The Ru–Tpy–Au nanoparticles thus display the expected electrochemistry.

In order to prepare a new type of polymer thin film containing metal nanoparticles and metal complex, pyrrole-modified Ru–Tpy–Au nanoparticles (Pyr–Ru–Tpy–Au) were prepared from the ligand-exchange reaction of Ru–Tpy–Au with thiol **2**. The UV-vis spectrum of Pyr–Ru–Tpy–Au solution in MeCN exhibited a characteristic MLCT absorption (λ_{max} = 483, 306 and 273 nm) and significant plasmon resonance (λ_{max} = ~510 nm) [Fig. 1(b)]. The TEM micrograph of Pyr–Ru–Tpy–Au indicated a particle size of 5.5 ± 1.0 nm. The ^{1}H NMR spectrum of Pyr–Ru–Tpy–Au in $CDCl_3$ showed that the peaks of the pyrrole groups appeared as broad peaks at δ 6.54 (2,5-pyrrole) and δ 5.94 (3,4-pyrrole).

The electropolymerization of Pyr–Ru–Tpy–Au was performed by cyclic voltammetry (CV). The first scan of the CV of Pyr–Ru–Tpy–Au in 0.1 M Bu_4NPF_6–MeCN at a GC electrode exhibited a single irreversible oxidation wave at Ep = +1.16 V (*vs.* Ag/0.1 M $AgNO_3$) which seems to overlap the oxidation peaks of the pyrrole group and the ruthenium(II)/(III) couple (Fig. 4). Repeat scans showed an increase in the redox-peak currents. After fifty scans, the electrode was rinsed copiously with solvent and dipped into fresh 0.1 M Bu_4NPF_6–MeCN solution. The CV of the poly(Pyr–Ru–Tpy–Au) film-modified GC electrode showed two irreversible peaks due to terpyridine at −1.58 and −1.91 V and one reversible redox peak due to the Ru(II)/(III) couple at +0.95 V (ΔEp = 114 mV) (Fig. 5). Thus, polypyrrole metal nanoparticles bearing a Ru-terpyridine complex are readily immobilized on metal electrode surfaces

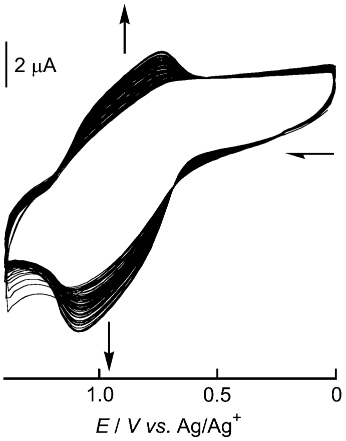

Fig. 4 Oxidative electropolymerization of Pyr–Ru–Tpy–Au by repeated potential scans on a GC electrode in 0.1 M Bu_4NPF_6–MeCN; scan rate 100 mV s^{-1}.

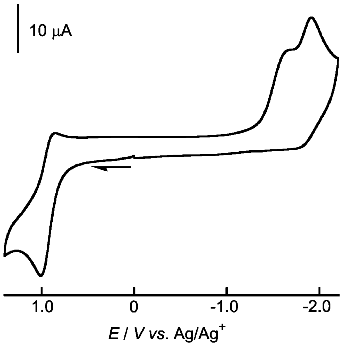

Fig. 5 Cyclic voltammogram of poly(Pyr–Ru–Tpy–Au) film-modified GC electrode in 0.1 M Bu_4NPF_6–MeCN; scan rate 100 mV s^{-1}.

by electrodeposition. This finding indicates the possibility for the immobilization of metal nanoparticles having several kinds of functional molecules on metal electrode surfaces. To our knowledge, this is the first example of polypyrrole nanocomposite films containing metal complex and metal nanoparticles.

Conclusion

We have demonstrated that the reduction of an Au(III) compound in the presence of the terpyridinylthiol results in the formation of terpyridinylthiolate monolayer-protected gold nanoparticles which are converted into ruthenium-coordinated terpyridine-functionalized gold nanoparticles. Thus metal complexation can be achieved without decomposition of the nanoparticles. The ligand-exchange reaction of Ru–Tpy–Au with a pyrrolylthiol gave Pyr–Ru–Tpy–Au bearing electropolymerizable sites and metal complex which provides a new type of poly(metal nanocomposite) films-modified electrode. Such ruthenium nanocomposite materials are of special interest, as they have applications to sensor devices, catalysis, and nanoelectronics. Further work is currently in progress in this and related areas.

Acknowledgements

This work was supported in part by the Grant-in-Aid for Scientific Research No. 15550044 from the Ministry of Education, Science and Culture, Japan.

Masayuki Ito, Takashi Tsukatani and Hisashi Fujihara*
Department of Applied Chemistry and Molecular Engineering Institute,
Kinki University, Kowakae, Higashi-Osaka 577-8502, Japan.
E-mail: h-fuji@apch.kindai.ac.jp

References

1 G. Schmid, *Clusters and Colloids*; VCH, Weinheim, 1994.
2 D. L. Feldheim and C. A. Foss, Jr., *Metal Nanoparticles*, Marcel Dekker, Inc., New York, 2002.
3 G. Schmid, *Nanoparticles*, Wiley-VCH, Weinheim, 2004.
4 M. Brust, M. Walker, D. Bethell, D. J. Schiffrin and R. Whyman, *J. Chem. Soc., Chem. Commun.*, 1994, 801.
5 A. C. Templeton, W. P. Wuelfing and R. W. Murray, *Acc. Chem. Res.*, 2000, **33**, 27.
6 H. Fujihara and H. Nakai, *Langmuir*, 2001, **17**, 6393.
7 A. Deronzier and J. C. Moutet, *Acc. Chem. Res.*, 1989, **22**, 249; D. Curran, J. Grimshaw and S. D. Perera, *Chem. Soc. Rev.*, 1991, **20**, 391; S. Sadki, P. Schottland, N. Brodie and G. Sabouraud, *Chem. Soc. Rev.*, 2000, **29**, 283.
8 A. Doron, E. Katz and I. Willner, *Langmuir*, 1995, **11**, 1313; A. N. Shipway, E. Katz and I. Willner, *ChemPhysChem*, 2000, **1**, 18; A. N. Shipway and I. Willner, *Chem. Commun.*, 2001, 2035.
9 Z. Peng, E. Wang and S. Dong, *Electrochem. Commun.*, 2002, **4**, 210.
10 K. Hata and H. Fujihara, *Chem. Commun.*, 2002, 2714.
11 (*a*) E. C. Constable and P. Harverson, *Inorg. Chim. Acta*, 1996, **252**, 9; (*b*) G. R. Newkome, E. He, L. A. Godinez and G. R. Baker, *J. Am. Chem. Soc.*, 2000, **122**, 9993 and references therein.
12 E. C. Constable and M. D. Ward, *J. Chem. Soc., Dalton Trans.*, 1990, 1405.
13 P. A. Adcock, F. R. Keene, R. S. Smythe and M. R. Snow, *Inorg. Chem.*, 1984, **23**, 2336.
14 The broadening effects of ^1H NMR signals in alkanethiolate-stabilized gold nanoparticles have been discussed[5].
15 M. M. Maye, W. Zheng, F. L. Leibowitz, N. K. Ly and C.-J. Zhong, *Langmuir*, 2000, **16**, 490; M. M. Maye and C.-J. Zhong, *J. Mater. Chem.*, 2000, **10**, 1895; T. Teranishi, S. Hasegawa, T. Shimizu and M. Miyake, *Adv. Mater.*, 2001, **13**, 1699.